Article

TRANSPARENT PROCESS OPEN ACCESS

THE EMBO JOURNAL

Sox2, Tlx, Gli3, and Her9 converge on Rx2 to define retinal stem cells *in vivo*

Robert Reinhardt[1,†,‡], Lázaro Centanin[1,*,‡], Tinatini Tavhelidse[1], Daigo Inoue[1], Beate Wittbrodt[1], Jean-Paul Concordet[2], Juan Ramón Martinez-Morales[3] & Joachim Wittbrodt[1,**]

Abstract

Transcriptional networks defining stemness in adult neural stem cells (NSCs) are largely unknown. We used the proximal *cis*-regulatory element (pCRE) of the *retina-specific homeobox gene 2* (*rx2*) to address such a network. Lineage analysis in the fish retina identified *rx2* as marker for multipotent NSCs. *rx2*-positive cells located in the peripheral ciliary marginal zone behave as stem cells for the neuroretina, or the retinal pigmented epithelium. We identified upstream regulators of *rx2* interrogating the *rx2* pCRE in a *trans*-regulation screen and focused on four TFs (Sox2, Tlx, Gli3, and Her9) activating or repressing *rx2* expression. We demonstrated direct interaction of the *rx2* pCRE with the four factors *in vitro* and *in vivo*. By conditional mosaic gain- and loss-of-function analyses, we validated the activity of those factors on regulating *rx2* transcription and consequently modulating neuroretinal and RPE stem cell features. This becomes obvious by the *rx2*-mutant phenotypes that together with the data presented above identify *rx2* as a transcriptional hub balancing stemness of neuroretinal and RPE stem cells in the adult fish retina.

Keywords de-differentiation; gene regulation; neural stem cells; retinal stem cells; transcriptional network

Subject Categories Development & Differentiation; Stem Cells; Transcription

DOI 10.15252/embj.201490706 | Received 1 December 2014 | Revised 21 March 2015 | Accepted 1 April 2015 | Published online 23 April 2015

The EMBO Journal (2015) 34: 1572–1588

Introduction

Post-embryonic neurogenesis relies on the activity of neural stem cells (NSCs) (Adolf *et al*, 2006; Zhao *et al*, 2008). The fish neural retina (NR) constitutes an ideal model to study embryonic and post-embryonic NSCs in their physiological environment. It consists of seven main cell types distributed in three nuclear layers, and all these cell types are added lifelong from retinal stem cells (RSCs) that reside in the peripheral ciliary marginal zone (CMZ) (Johns, 1977; Lamba *et al*, 2008; Centanin *et al*, 2011). The CMZ also contributes to the retinal pigmented epithelium (RPE), a monolayer of pigmented cells surrounding and synchronously growing with the NR (Johns, 1977; Amato *et al*, 2004a; Moshiri *et al*, 2004; Centanin *et al*, 2011). As an attractive model for life-long neurogenesis as well as growth of the RPE, the CMZ has been extensively studied in fish, frog, and chicken (Amato *et al*, 2004b; Raymond *et al*, 2006; Lamba *et al*, 2008).

The lack of genetic tools to follow lineages in these species, however, was a long-lasting limitation to validate putative RSC-specific markers, which in turn prevented understanding the regulatory framework that generates and maintains this stem cell fate. In medaka, retinal multipotent NSCs were identified by their virtue to form arched continuous stripes (ArCoS) via cell transplantation at early embryonic stages (Centanin *et al*, 2011) and by inducible recombination in late embryonic and post-embryonic stages (Centanin *et al*, 2014). These experiments demonstrated that the maintenance of the NR and the RPE is achieved by independent RSCs located in the CMZ.

How the function of NSCs is maintained in the CNS remains largely unknown. Two of the best-studied factors expressed by post-embryonic NSCs in other niches are Sox2 and Tlx, which have been shown to be crucial for the self-renewal and differentiation of NSCs (Monaghan *et al*, 1995; Graham *et al*, 2003; Shi *et al*, 2004). Furthermore, fate-mapping studies showed that *sox2* (Suh *et al*, 2007) and *tlx* (Liu *et al*, 2008) are markers for multipotent stem cells in the mammalian brain. Identifying target genes regulated by NSC-determining TFs is crucial for the understanding of the molecular and signaling pathways underlying adult neurogenesis. Previously, Sox2 has been demonstrated to bind and regulate the *gfap* regulatory element (Cavallaro *et al*, 2008). Target genes regulated by Tlx include cell cycle regulators *p21* and *pten* (Sun *et al*, 2007). The function of Tlx is context dependent; inhibition of target genes relies on the interaction with HDACs (Sun *et al*, 2007), while Tlx can also act as activator of transcription (Iwahara *et al*, 2009).

1 Centre for Organismal Studies (COS) Heidelberg, Heidelberg University, Heidelberg, Germany
2 Muséum National d'Histoire Naturelle, Paris, France
3 Centro Andaluz de Biología del Desarrollo (CSIC/UPO/JA), Sevilla, Spain
*Corresponding author. Tel: +49 6221 546253; E-mail: lazaro.centanin@cos.uni-heidelberg.de
**Corresponding author. Tel: +49 6221 546499; E-mail: jochen.wittbrodt@cos.uni-heidelberg.de
‡These authors contributed equally to this work
†Present address: Developmental Genetics, Department of Biomedicine, University of Basel, Basel, Switzerland

Characterizing a NSC regulatory network crucially depends on the identification of a reliable molecular marker and the main *cis*-acting regulators controlling its proper expression pattern. Here, we followed a long-term lineage analysis to identify the transcription factor (TF) *retina-specific homeobox gene-2* (*rx2*) as a *bona fide* marker for multipotent adult RSCs in the post-embryonic medaka CMZ. We show that individual $rx2^+$ RSCs give rise to progeny contributing either to NR or to RPE. Next, we identified TFs acting upstream of *rx2* in a *trans*-regulation assay using the *rx2* proximal *cis*-regulatory element (pCRE) and characterize *sox2*, *tlx*, *gli3*, and *her9* as transcriptional modulators of stem cell features in the post-embryonic fish retina. Clonal expression of *sox2* or *tlx* induces RSC-specific characteristics, including ectopic *rx2* expression in differentiated neurons of the central retina. Conversely, conditional clonal gain of Gli3 or Her9 function leads to *rx2* repression and inhibits stem cell proliferation in the post-embryonic CMZ. We also identify and validate the *cis*-regulatory motifs within the proximal *rx2* pCRE that activate expression in the peripheral most CMZ, and repress expression in the adjacent RPE. Additionally, we show that the *rx2* expression levels resulting from this transcriptional network establish the balance between NR and RPE stem cells. Our *in vitro* and *in vivo* results provide evidence for the importance of direct TF-DNA binding for proper spatial *rx2* expression in RSCs. Taken together, we present a regulatory framework of TFs that establish, expand, and restrict RSC features in the post-embryonic retina and demonstrate a crucial function of Rx2 in the definition of retinal stem cell types.

Results

Rx2 labels the most peripheral cells in the ciliary marginal zone of the medaka retina

To specifically target RSCs in the CMZ, we followed a candidate gene approach and systematically searched for genes and their regulatory regions with expression confined to the CMZ. Both in amphibians and fish, the *retina-specific homeobox gene-1* and *retina-specific homeobox gene-2* (*rx1* and *rx2* respectively) are expressed in the peripheral CMZ at embryonic and post-embryonic stages (Locker *et al*, 2006; Raymond *et al*, 2006; Borday *et al*, 2012). In medaka, *rx2* is first expressed in the undifferentiated retinal progenitor cells (RPCs) that form the optic vesicle (Loosli *et al*, 1999). At later stages, when the fish retina already contains all the main cell types and is functionally active, *rx2* expression is confined to photoreceptors (cones and rods in the outer nuclear layer, ONL), to the Müller glia cells, and to the peripheral most part of the CMZ, as revealed by *in situ* hybridization and immunostaining (Fig 1A and B) (Sinn *et al*, 2014). Medaka transgenic lines in which 2.4 kb of the proximal *rx2* pCRE control the expression of a reporter fluorescent protein (FP) (*rx2*::H_2B-mRFP and *rx2*::Tub-GFP) (Martinez-Morales *et al*, 2009; Inoue & Wittbrodt, 2011) (Fig 1B and C; Supplementary Fig S1) exhibit the same expression pattern, indicating that the 2.4-kb *rx2* pCRE contains the regulatory cues driving *rx2* expression to those cell types.

The post-embryonic medaka retina grows outwards, with the RSCs located in the most peripheral domain of the CMZ (Centanin *et al*, 2011). A close analysis at *rx2*::H_2B-mRFP transgenic juveniles revealed that $rx2^+$ cells locate to the peripheral most domain of the CMZ (Fig 1C), suggesting that Rx2 constitutes a marker for RSCs. On the central side of the CMZ, differentiating $Atoh7^+$ cells demarcate the boundary between the central most domain of the CMZ and the differentiated, layered retina (Fig 1C) (Del Bene *et al*, 2007; Cerveny *et al*, 2010). As expected for stem cells, $rx2^+$ cells in the post-embryonic CMZ barely incorporate the thymidine analog bromodeoxyuridine (BrdU) when applied in short pulses (Supplementary Fig S2A) and similarly, there is only partial overlap with proliferation markers like phospho-histone H3 (pHH3) and proliferating cell nuclear antigen (PCNA) (Supplementary Fig S2B and C). Most of the $BrdU^+$, $PCNA^+$, and/or $pH3^+$ cells of the CMZ map to the progenitor domain, between the $rx2^+$ cells and the $Atoh7^+$ cells.

In medaka, transplantation of $EGFP^+$ cells from the $Wimbledon^{+/-}$ line (a transgenic line that expresses EGFP ubiquitously during the entire life of the fish) (Centanin *et al*, 2011) into an unlabeled blastula results in fish with mosaic retinae. In these chimeric fish, RSCs were addressed by their property to form ArCoSs, which are continuous clonal strings of $EGFP^+$ cells consisting of differentiated neurons and glia at central positions, and undifferentiated cells in the peripheral domain. We reasoned that if $rx2^+$ cells were indeed RSCs, all the ArCoSs should contain $rx2^+$ cells located at the most peripheral position of the clone. We therefore transplanted $Wimbledon^{+/-}$, *rx2*::H_2B-mRFP donor cells into wild-type hosts and consistently found $rx2^+$ cells at the peripheral tip in all resulting ArCoSs (Fig 1D and E). Thus, the expression domain of $rx2^+$ and the relative position of $rx2^+$ cells within an ArCoS match the expected location of RSCs and suggest that $rx2^+$ is a RSC marker in the mature medaka retina.

Rx2 is a molecular marker of adult RSCs

The ultimate validation of $rx2^+$ as a stem cell marker is to follow the lineage of an individual $rx2^+$ cell in the medaka CMZ during several months of post-embryonic life. The Gaudí toolkit allows single-cell labeling and lineage analysis in medaka (Centanin *et al*, 2014), based on Cre/LoxP-mediated recombination. When fish bearing a ubiquitous Cre driver and a Gaudí reporter are induced for stochastic recombination, single RSCs generate induced ArCoSs (*i*ArCoSs) of the same characteristics than the ArCoSs generated by transplantation (Centanin *et al*, 2014).

To address if *rx2* marks RSCs and if the progeny of an $rx2^+$ cell in the CMZ forms an *i*ArCoS, we generated a transgenic line expressing a tamoxifen-inducible Cre recombinase under the control of the well-characterized 2.4-kb *rx2* pCRE (*rx2*::^{ERT2}Cre). We induced Cre recombinase within the *rx2* expression domain to trigger recombination in the ubiquitously expressed four-color reporter cassette ($Gaudí^{2.1}$) (Centanin *et al*, 2014). Tamoxifen induction of *rx2*::^{ERT2}Cre, $Gaudí^{2.1}$ at 10 dpf resulted in the specific labeling of individual $rx2^+$ cells, as shown by stochastic expression of FPs labeling single photoreceptors, Müller glia, and peripheral cells in the CMZ (Fig 2A).

Long-term lineage experiments showed that $rx2^+$ cells formed *i*ArCoSs and thus indeed represent RSCs (n = 162 red-colored *i*ArCoSs distributed over 7 retinae, ranging from 15 to 31 *i*ArCoSs per retina, average 23.1 *i*ArCoSs/retina) (Fig 2B). Lineage analyses indicate as well that every single $rx2^+$ post-embryonic NR stem cell analyzed is multipotent, equivalent to ArCoS-forming RSCs in transplantation experiments. Each *i*ArCoS contains the full repertoire of differentiated retinal cell types of the NR (n= 125 NR *i*ArCoSs) (Fig 2C).

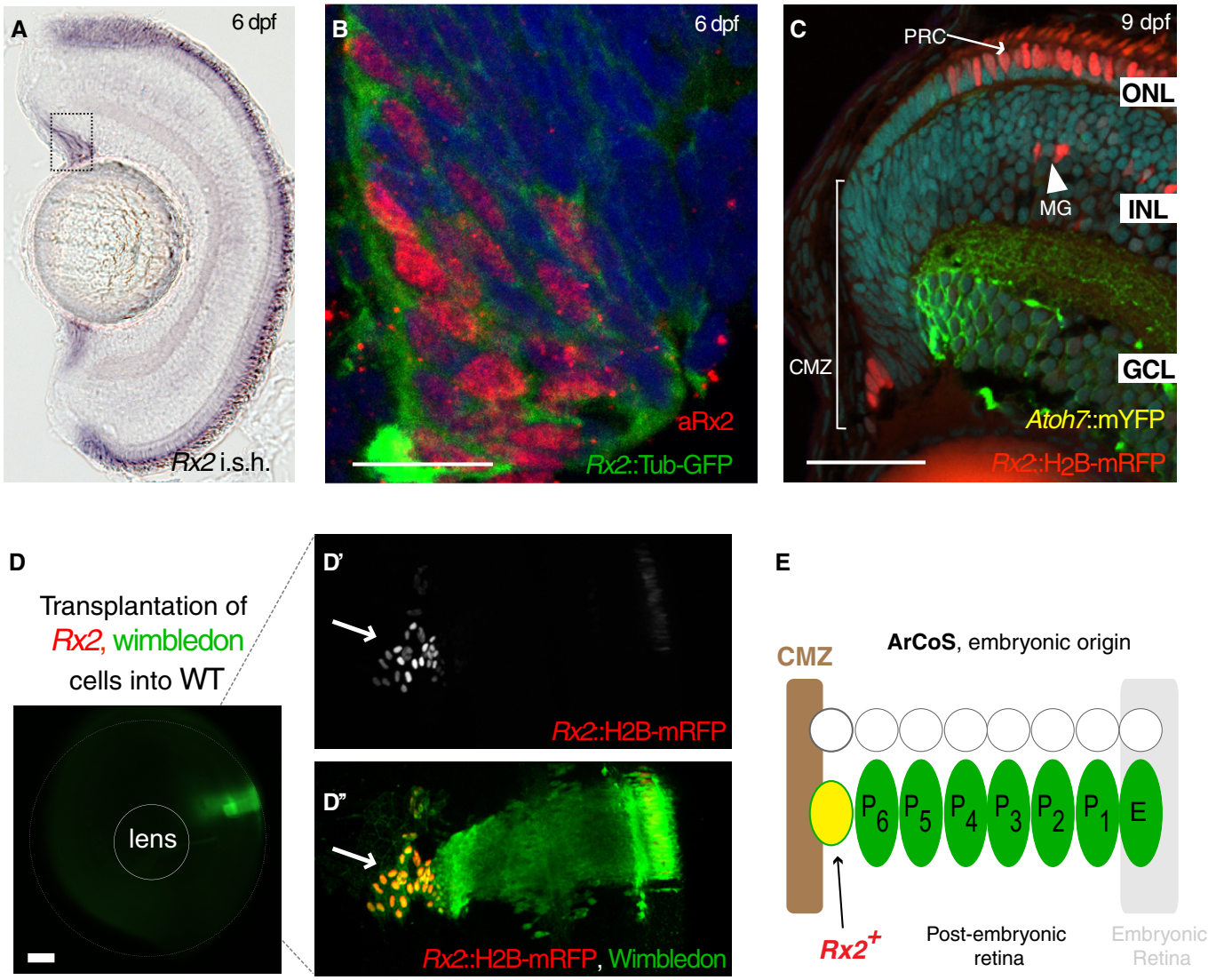

Figure 1. *Rx2* functions as retinal stem cell (RSC) marker.

A *rx2* mRNA is strongly detected in the peripheral CMZ of juvenile medaka (black box).

B Expression analysis of boxed area in (A). Transgenic reporter (*rx2*::Tub-GFP in green) overlaps with Rx2 immunostaining (in red).

C Cross-section of a transgenic *rx2*::H_2B-mRFP juvenile medaka. $rx2^+$ cells are located in the most peripheral domain of the CMZ (bracket), limited centrally by *Atoh7*::mYFP. $rx2^+$ cells in the central retina are Müller glia (arrowhead) and photoreceptors (arrow).

D, E Transplantation of *rx2*::H_2B-mRFP, *Wimbledon* cells into wild-type medaka demonstrates that $rx2^+$ cells represent the most peripheral cells in an ArCoS.

Data information: Scale bars represent 25 μm in (B), 50 μm in (C), and 100 μm in (D).

Remarkably, $rx2^+$ RSCs as a population give rise to *i*ArCoSs in both the NR and the RPE (Fig 2B). An individual $rx2^+$ RSC, however, can be a stem cell either for the NR or for the RPE ($n = 25$ NR *i*ArCoSs and 136 RPE *i*ArCoS distributed over 8 retinae, 98.5% of independent *i*ArCoSs).

Identification of Sox2, Tlx, Gli3, and Her9 as transcriptional regulators in control of retinal stemness

To identify genes controlling RSC features, we followed a high-throughput *trans*-regulation screen (Souren *et al*, 2009) to systematically detect factors operating on the *rx2* pCRE. The *trans*-regulation screen is based on two nested screens. In a first step, it employs a high-throughput luciferase assay based upon the co-expression of an *rx2* pCRE reporter construct driving firefly luciferase together with individual full-length candidate TFs (Fig 3A). This cell culture-based assay allows transcriptome scale analyses and has been used reliably to identify so far unknown upstream regulators (Souren *et al*, 2009). We took advantage of the relatively short 2.4-kb proximal *rx2* CRE sufficient to recapitulate the *rx2* expression pattern and assayed more than one thousand individual full-length cDNA clones, which represented a large complement of all putative medaka TFs. We controlled for transfection efficiencies in a dual luciferase-based screen in cultured cells through co-transfection of a

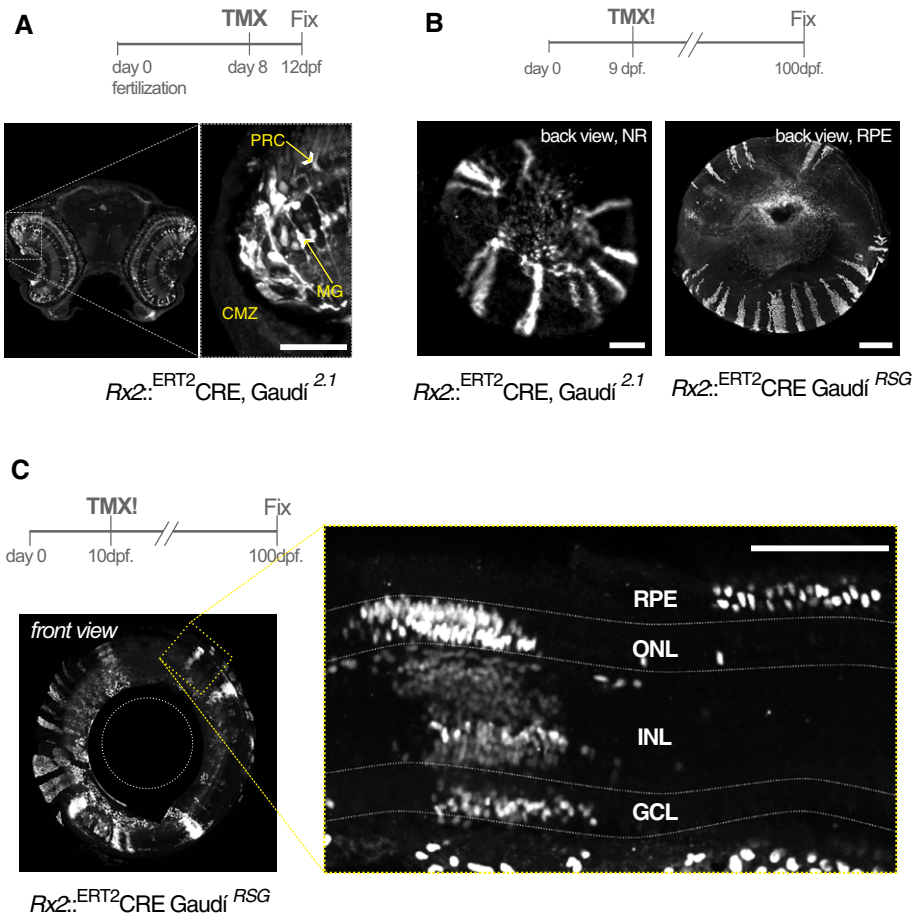

Figure 2. Individual *rx2*-positive cells are stem cells for the neural retina (NR) or the retinal pigmented epithelium (RPE).

A The stochastic expression of fluorescent proteins (FPs) allows single-cell labeling within the $rx2^{+}$ expression domain.

B ArCoS generation by individual $rx2^{+}$ cells defines *rx2* as a marker for RSCs for the NR, and the RPE. *rx2* labels individual RSCs for (left) the NR and (right) the RPE.

C All $rx2^{+}$ cells forming ArCoSs in the NR are multipotent, generating all NR cell types.

Data information: CMZ, ciliary marginal zone; GCL, ganglion cell layer; INL, inner nuclear layer; MG, Müller glia; ONL, outer nuclear layer; PRC, photoreceptor cell. Scale bars represent 50 μm (A) and 100 μm (B, C).

control plasmid encoding *Renilla* luciferase (Fig 3A). To exclude potential false positives, we performed a secondary, nested, whole-mount *in situ* screen to analyze the expression pattern of putative candidate TFs relative to *rx2* by a semi-automated whole-mount *in situ* hybridization approach (Quiring *et al*, 2004). We eventually selected activating or repressing candidates based on their co-expression with or adjacent to *rx2* in the juvenile CMZ.

This nested screening pipeline delivered clear candidates from the more than one thousand TFs analyzed: *sox2* was the top activator, while *gli3* and *her9* (a medaka *Hes1* ortholog) showed the strongest repressive activities. *tlx*—not initially present in the full-length TF library—showed a strong activation of the *rx2* pCRE (Fig 3C) and was assayed in a parallel candidate screen because of its role in mouse NSCs (Yu *et al*, 1994; Monaghan *et al*, 1995; Shi *et al*, 2004). To test whether Sox2, Tlx, Her9, and Gli3 regulate *rx2* transcription in a concentration-dependent manner, we performed dual luciferase assays with increasing amounts of the respective TF cDNA. For Sox2 (Fig 3B), we observed the activation of relative luciferase activity in a dose-dependent manner. Likewise, for Tlx (Fig 3C) activation of transcription peaked with the highest cDNA concentration (160 ng), implicating *tlx* as an activator of *rx2* expression. Conversely, stepwise increase of Her9 resulted in the gradual reduction of reporter expression (Fig 3D). Interestingly, Gli3-mediated repression of *rx2* pCRE activity was strongest at the lowest Gli3 concentration (Fig 3E), while increasing cDNA amounts led to a gradual reduction of its repressive potential.

Next, we addressed the expression patterns of *sox2*, *tlx*, *gli3*, and *her9* with respect to their putative target gene *rx2* in the juvenile CMZ by two-color fluorescent whole-mount *in situ* hybridization (WISH). All four regulators are expressed in nested domains that partially overlap with the *rx2* expression domain in the CMZ. We detected transcripts of the pan-neural determinant *sox2* throughout the CMZ overlapping with the Rx2 expression domain (Fig 3F–H). *tlx* and *her9* were both expressed in the central CMZ where they partially overlapped with the *rx2* expression domain (Fig 3I–N). *gli3*

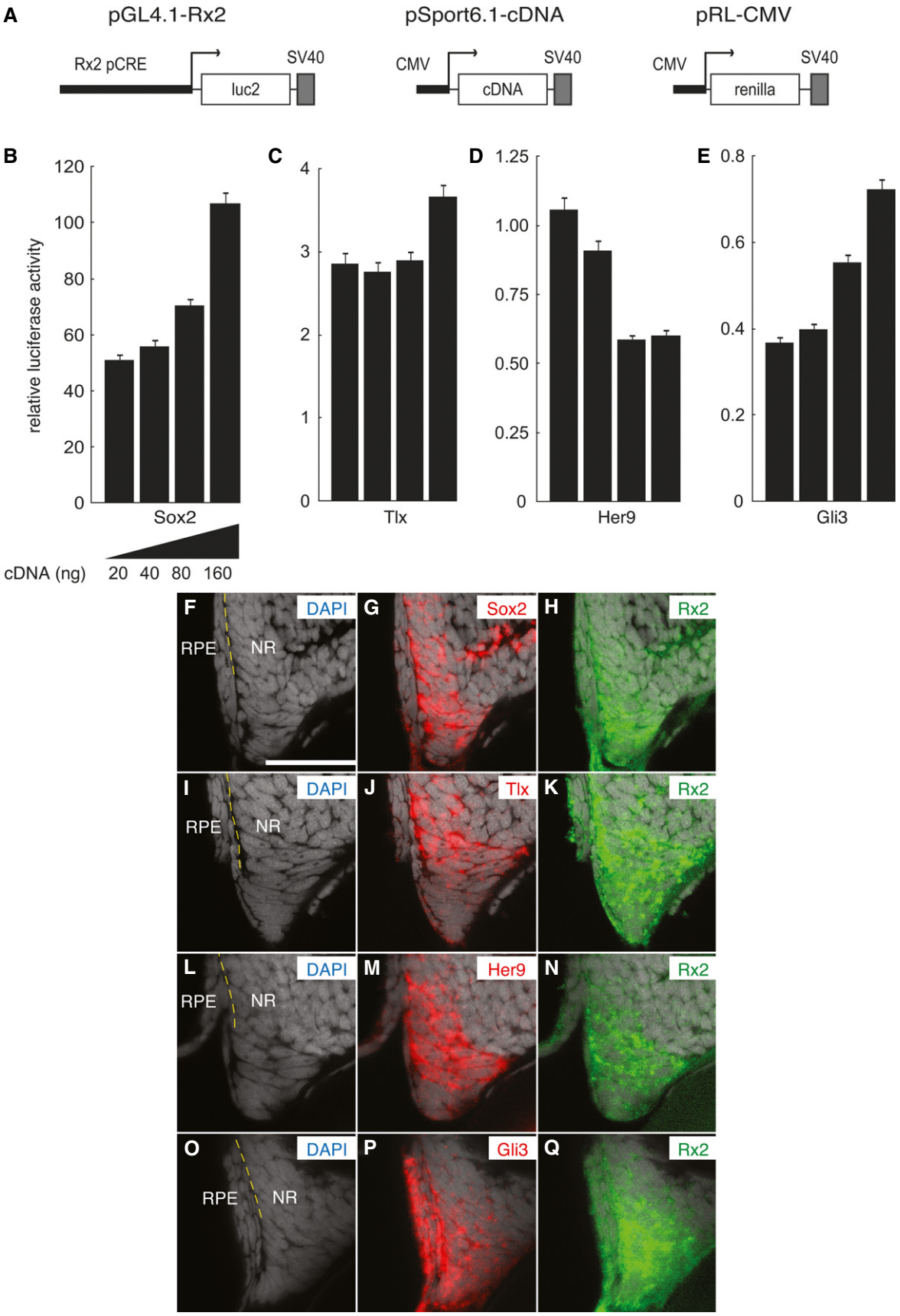

Figure 3.

Figure 3. Transcriptional regulators of *rx2* are expressed in the post-embryonic CMZ.

A A luciferase-containing vector (pGL4.1-*rx2*) was co-transfected with individual cDNA clones (pSport6.1-cDNA) and an internal control (pRL-*CMV*) to measure the transcriptional response of the *rx2* pCRE in BHK cells.

B–E Dual luciferase assays show dose-dependent activation and repression of *rx2 cis*-regulatory activity in BHK cells. All values were normalized against the luminescence recorded in cells transfected with pCS2+ and reporters only. Values indicate averages of four replicates. Error bars indicate standard deviation.

F–Q Confocal stacks of two-color WISHs with probes against *sox2* (G, red), *tlx* (J, red), *her9* (M red), *gli3* (P, red), and *rx2* (H, K, N, Q, green) on medaka hatchlings. Vibratome sections show the distinct expression patterns of *sox2*, *tlx*, *her9*, and *gli3*, which partially overlap with the expression of *rx2* in the peripheral CMZ. Dashed line demarcates boundary between RPE and NR. Scale bar represents 25 μm.

transcripts were found in the peripheral CMZ overlapping with *rx2* expression and were also found in the adjacent RPE (Fig 3O–Q). Out of all the *rx2* regulators identified in the *trans*-regulation screen, *gli3* was the only factor expressed in the peripheral RPE adjacent to the CMZ.

Gli3 and Her9 antagonize stem cell features *in vivo*

To test whether these candidate factors regulate *rx2* expression *in vivo*, we employed a conditional clonal analysis in the post-embryonic retina. For this purpose, we adopted a hormone-inducible binary gene expression system, which consists of a TF (LexPR) that upon hormone induction will dimerize and bind to the corresponding promoter element (LexOP) to activate the expression of following genes of interest (Emelyanov & Parinov, 2008). We established transgenic lines expressing LexPR in the CMZ under the control of the *rx2* pCRE (Fig 4A). Upon addition of mifepristone (RU-486), dimerization and LexOP-dependent transcription were initiated (Fig 4B). By limited exposure to the hormone, we triggered mosaic expression of *gli3* or *her9* (and the co-expression of a fluorescent reporter protein) within the very specific Rx2 domain in the CMZ and Müller glia cells as well as in mature photoreceptor cells. This system allows co-expressing fluorescent reporter proteins and the gene of interest with high efficiency (up to 90%). Consequently, the analyses based on the expression of the fluorescent reporter are conservative and always underestimate the effects of the gene of interest.

To assess the repressive potential of *gli3* and *her9*, respectively, on the expression of *rx2 in vivo*, we targeted their clonal expression to the peripheral *rx2*$^+$ CMZ. Gain-of-function clones were highlighted by the co-expression of nuclear FPs (Fig 4F and I). The expression of Rx2 protein was determined by antibody staining and analyzed automatically by a threshold-based segmentation algorithm. The repression of the pCRE of *rx2* by Her9 and Gli3 in the CMZ in this experiment not only affects the endogenous Rx2 but also the ectopic expression of the repressors. Consequently, we consistently underestimated the repressive potential Her9 and Gli3 on *rx2*. Six days after the clonal induction of Gli3 in the peripheral CMZ (*rx2*::LexPR *LexOP*::Gli3 *LexOP*::H_2B-EGFP), Rx2 protein was lost in 39.4% of the induced *gli3*$^+$ cells (n = 13/33) in the CMZ (compare Fig 4C–E to F–H). Similarly, 20% of the induced *her9*$^+$ cells (*rx2*::LexPR *LexOP*::Her9 *LexOP*::H_2B-EGFP) (n = 7/35) had lost Rx2 expression (compare Fig 4C–E to I–K), whereas the GFP alone had no effect on the *rx2* expression (n = 1/34) (Fig 4C–E). These findings are in support of the hypothesis of Her9 and Gli3, confining *rx2* expression as repressors in the central and peripheral domain of the CMZ.

Since both Gli3 and Her9 showed the ability to repress *rx2* expression *in vivo*, we next addressed the impact of ectopic *gli3*/*her9* expression on the proliferative capacity of RSCs in the CMZ. PCNA staining, which labels S-phase cells within the CMZ, was low only in very few cells in the CMZ of GFP control retinae (n = 3/38). Conversely, PCNA expression was affected in the *gli3* and *her9* gain-of-function clones at rates comparable to those observed for the repression of Rx2. PCNA was severely affected in *gli3* gain-of-function clones (n = 39/106) (compare Fig 4L–N to O–Q) or *her9* gain-of-function clones (n = 21/64) (compare Fig 4L–N to R–T). Taken together, these results indicate that ectopic clonal *gli3* and *her9* expression in the CMZ represses *rx2* expression and impacts negatively on the proliferation of RSCs.

Sox2 and Tlx promote *rx2* expression

Since our *in vitro* characterization and the overlapping expression pattern of *sox2* and *tlx* with *rx2* consistently argued for an activating function of *sox2* and *tlx*, we tested the consequences of acute clonal activation of *sox2* (*cska*::LexPR *LexOP*::*sox2*) and *tlx* (*cska*::LexPR *LexOP*::*tlx*) gain-of-function (Fig 5A). Gain-of-function clones were marked by the expression of red FPs (*LexOP*::cherry), encoded by co-injected reporter plasmids. In combination with the ubiquitous *cska* promoter (Grabher *et al*, 2003), this approach allowed clonal, mosaic expression throughout all three nuclear layers of the differentiated retina (Fig 5B).

We first examined the consequences of Sox2 and Tlx co-expression on *rx2* promoter activity *in vivo*. The transgenic reporter line expressed FP under the *rx2* pCRE (*rx2*::Tub-GFP). The combined expression of *sox2* and *tlx* resulted in strong *rx2* reporter activation (n = 40/48) in all three nuclear layers (Fig 5C and D). Individual clonal mis-expression of *sox2* (n = 32/48) (Supplementary Fig S3A–D) or *tlx* (n = 142/173) (Supplementary Fig S3F–I) also resulted in ectopic *rx2* reporter activation with high efficiency. To corroborate that *sox2* and *tlx* activate endogenous *rx2* expression *in vivo*, we combined WISH and immunohistochemistry in whole-mount preparations. Clones expressing *sox2* (n = 53/62) (Supplementary Fig S3E–E‴) or *tlx* (n = 34/56) (Supplementary Fig S3J–J‴) efficiently triggered the ectopic expression of endogenous *rx2* mRNA, which was never detected in controls.

We next asked whether the clonal activation of *sox2* or *tlx* was sufficient to trigger the ectopic induction of RSC features. While control clones in central retinal cell types never showed proliferating activity, the expression of Sox2 (n = 7/11) (Fig 5E–I) or Tlx (n = 3/23) (Fig 5J–N) resulted in the re-acquisition of proliferative features as indicated by PCNA staining. PCNA$^+$ clones were observed in the INL and ONL, indicating that de-differentiation and re-initiation of proliferation were not restricted to one particular type of retinal neurons. Together, these results revealed that both *sox2* and *tlx* induce the endogenous expression of *rx2* *in vivo*, and re-activate the proliferative potential of post-mitotic cells.

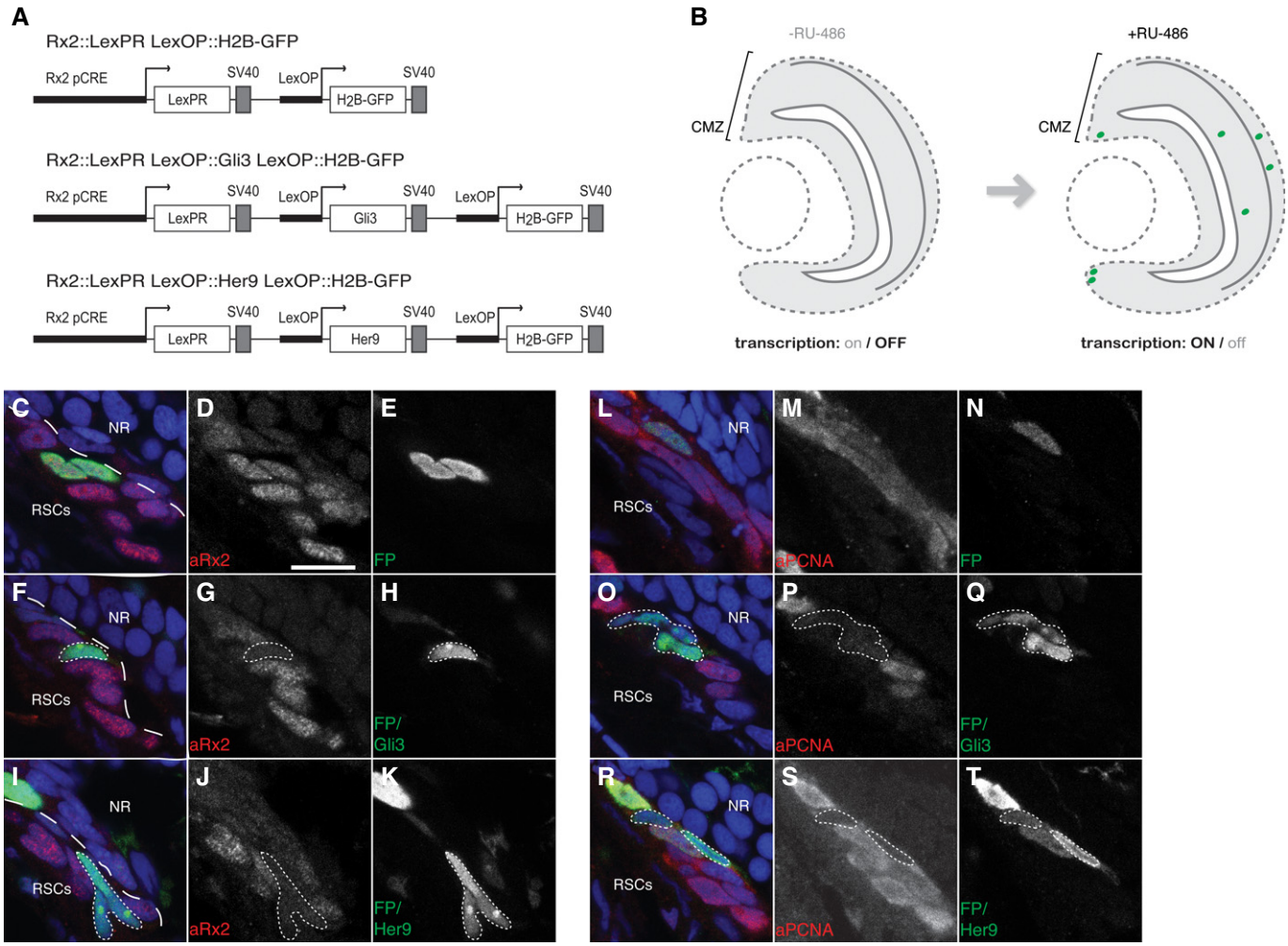

Figure 4. Clonal gain of *gli3* or *her9* restricts *rx2* expression and proliferation in the CMZ.

A Transgenic hormone-inducible lines for overexpression of *gli3*, *her9*, and H_2B-EGFP (control).

B Addition of RU-486 induces mosaic overexpression of transgenes in the Rx2 domain.

C–K The cross-sections of transgenic control embryos (*rx2*::LexPR *LexOP*::H_2B-EGFP, C–E) were compared to retinae mis-expressing *gli3* (*rx2*::LexPR *LexOP*::Gli3 *LexOP*::H_2B-EGFP, F–H) and *her9* (*rx2*::LexPR *LexOP*::Her9 *LexOP*::H_2B-EGFP, I–K) in the *rx2* domain 9 days post-fertilization (dpf). Sustained clonal gain of Gli3 (F–H) or Her9 (I–K) inhibited *rx2* expression as indicated by loss of Rx2 protein (in red). Scale bars represent 10 μm.

L–T Gli3 (O–Q) or Her9 (R–T) gain-of-function clones frequently lacked PCNA protein compared to control cells (L–N). Dashed lines demarcate RSC domain in the CMZ. Dotted outlines highlight affected cells. Scale bars represent 10 μm.

Sox2 and Gli3 regulate *rx2* expression through direct protein–DNA interaction with the *rx2* pCRE

Our analysis showed that *sox2* and *tlx* trigger some RSC features in differentiated retinal cells, while *gli3* and *her9* constrain *rx2* expression and stem cell proliferation in the CMZ. To investigate whether these effects are mediated by direct *trans*-regulation on the *rx2* pCRE, we carried out a combination of *in vitro* and *in vivo* analyses.

We started by performing an evolutionary footprinting analysis on the *cis*-regulatory elements present in the *rx2* pCRE. We identified evolutionarily conserved binding sites for Gli (Sasaki *et al*, 1997) and for Sox (Danno *et al*, 2008), the strongest repressor and activator in the *in vitro* assay, respectively (Fig 6A). Direct interaction between Sox2 and the *Rax* promoter has been demonstrated in *Xenopus* (Danno *et al*, 2008). To test whether Sox2 binds to the predicted, putative Sox-binding site in the medaka *rx2* pCRE, we next performed electromobility shift assays (EMSA). Sox2 showed sequence-specific binding to the *rx2* pCRE, which was weakened upon mutation of the predicted Sox TFBS (Fig 6B). Similarly, the specific affinity of Gli3 protein to the *rx2* pCRE was abolished when we tested the *rx2* pCRE lacking the Gli-binding motif (Fig 6B).

Next, we investigated whether the transcriptional regulation of *rx2* expression is impaired upon mutation of the identified Sox or Gli TFBSs. For this, we employed the luciferase *trans*-regulation assay and compared the transcriptional activity of *rx2* pCREs with mutated Sox or Gli motifs (*rx2* pCRE mtSox and *rx2* pCRE delGli) to the corresponding wild-type activity (Fig 6C). The transcriptional activation of the *rx2* pCRE through the predicted Sox2-binding site was severely attenuated by the introduction of mutations into the

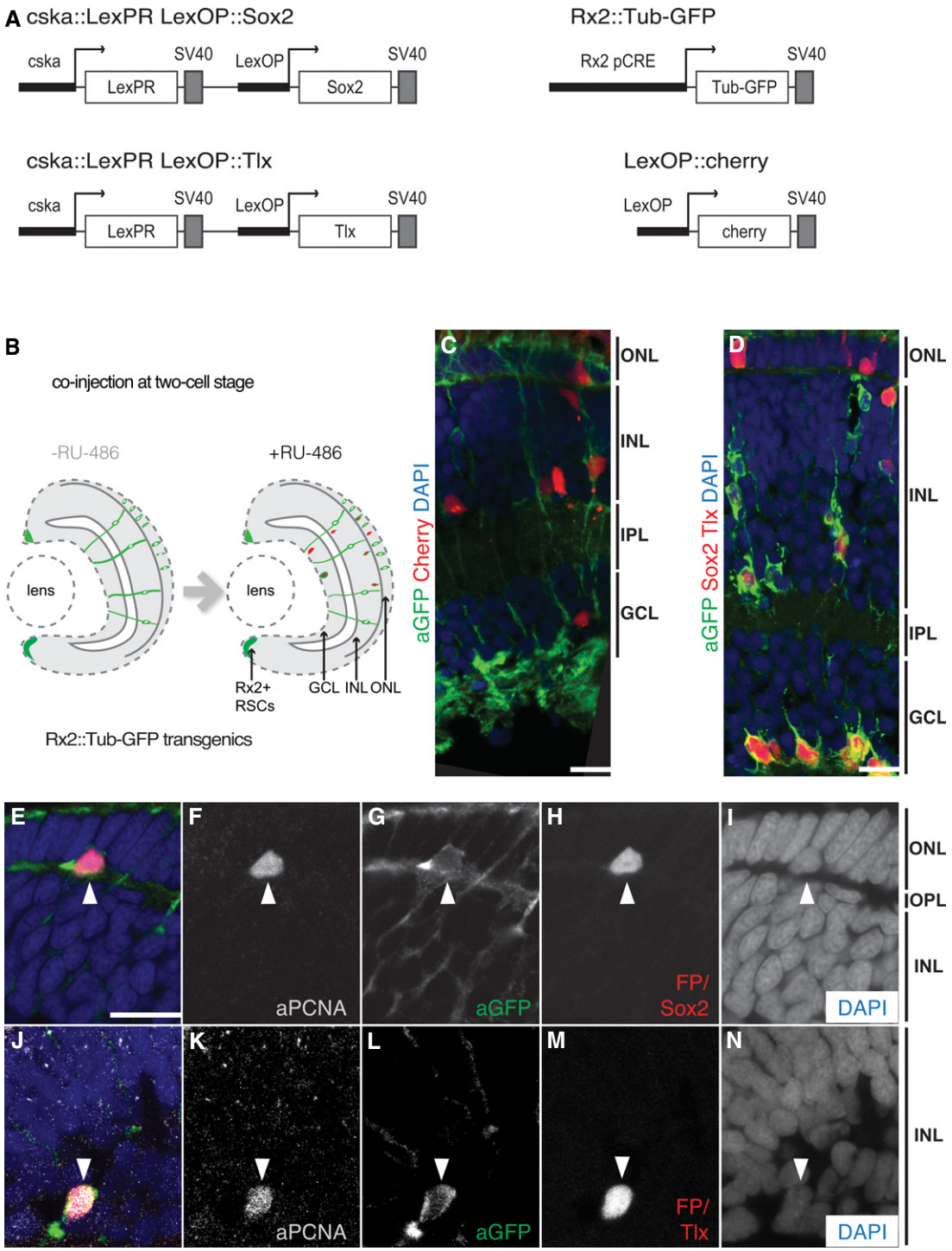

Figure 5. Expression of *sox2* or *tlx* promotes stem cell features in terminally differentiated neurons.

A Hormone-inducible expression plasmids for co-injection into transgenic *rx2*::Tub-GFP or wild-type embryos.

B Positive clones were traced by the expression of FPs (*LexOP*::Cherry), encoded by co-injected reporter plasmids. In combination with the ubiquitous *cska* promoter, this approach facilitated mosaic expression throughout all three nuclear layers in transgenic *rx2*::Tub-GFP embryos. Expression of the candidate factors was hormonally induced (4 dpf) when the majority of cells in the central retina (CR) had exited the cell cycle and already differentiated into the neuronal and glial cell types.

C, D Compared to control (C), combined expression of *tlx* and *sox2* (D) triggered ectopic *rx2* pCRE activation.

E–N In addition to ectopic *rx2* expression, PCNA protein was detected upon *sox2* or *tlx* expression at 7 dpf.

Data information: White arrowheads point to representative co-expressing cells. GCL, ganglion cell layer; INL, inner nuclear layer; IPL, inner plexiform layer; ONL, outer nuclear layer; OPL, outer plexiform layer; RSCs, retinal stem cells. Scale bar represents 10 μm.

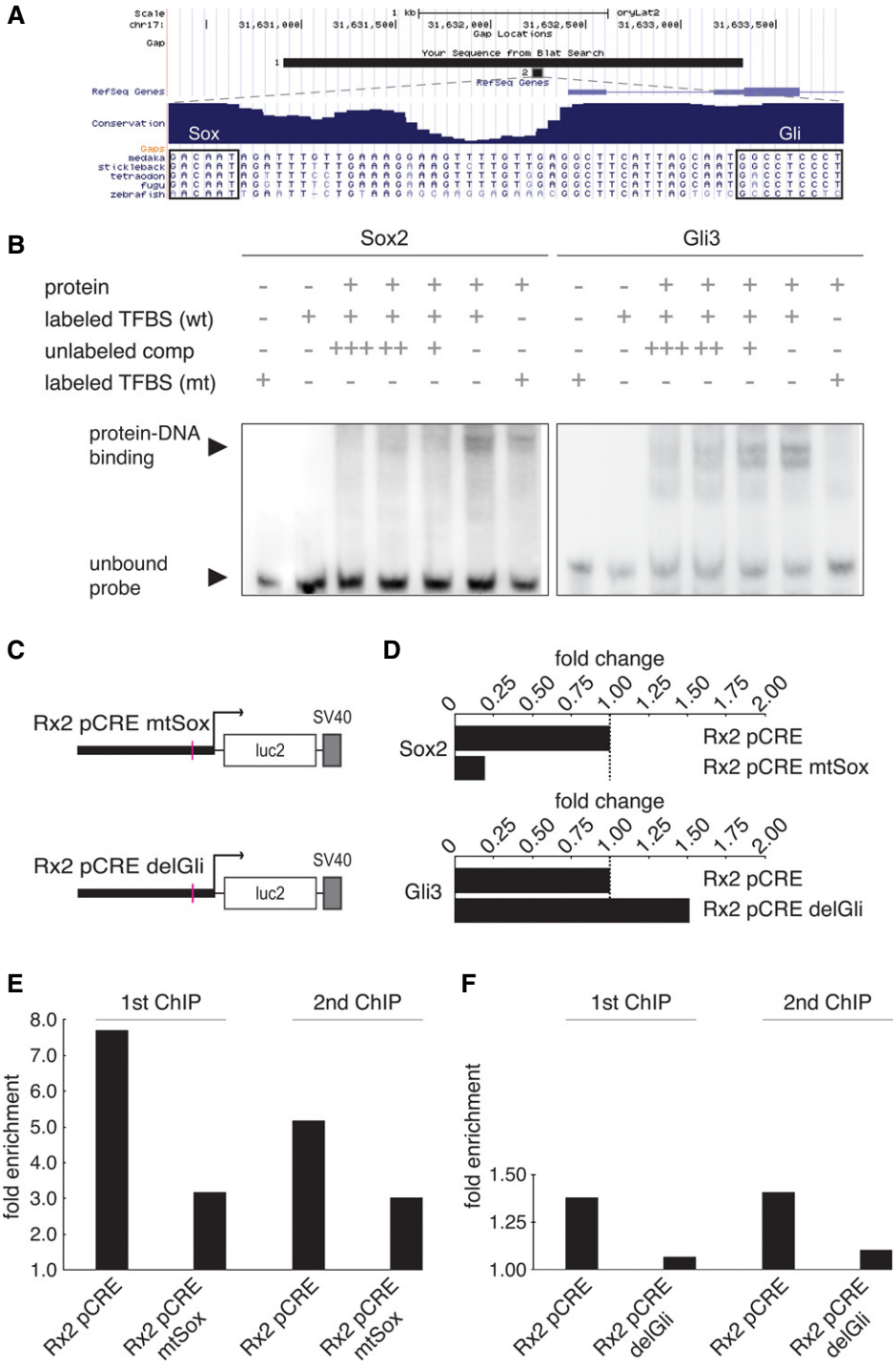

Figure 6. The *rx2* pCRE contains conserved Sox- and Gli-binding sites, which interact with Sox2 and Gli3 proteins.

A Result of BLAT search for the 2.4-kb medaka *rx2* pCRE using the UCSC Genome Browser. The region, which contains the predicted Sox- and Gli-binding sites, is conserved. Blue peaks indicate conservation of coding and non-coding DNA.

B Sox2 and Gli3 proteins bind to predicted sites within the *rx2* pCRE. The DNA–protein interaction is reduced/abolished through mutations introduced in the binding motifs.

C, D Reporter vectors carrying mutations (indicated by pink bars) in Sox (*rx2* pCRE mtSox) or Gli (*rx2* pCRE delGli) motifs in *rx2* pCRE followed by firefly luciferase were co-transfected with 20 ng of *sox2* or *gli3* cDNA. Results of dual luciferase assays show that relative luciferase activity is reduced with *rx2* pCRE mtSox compared to *rx2* pCRE (C). Repression mediated by Gli3 is attenuated with *rx2* pCRE delGli (D). Values were first normalized against the luminescence recorded in cells transfected with pCS2+ and reporters only (averages of four replicates). Normalized averages of modified *rx2* pCREs (mtSox or delGli) were then normalized against the respective averages of wild-type *rx2* pCRE.

E, F Fold enrichments of two independent ChIP-PCR assays for Sox2 (E) and Gli3 (F) on *rx2* pCRE. Enrichments for Sox2 and Gli3 TFBSs were normalized against control luciferase fragments (summarized in Supplementary Table S1).

Sox-binding site (from 50.99 ± 2.19 to 9.93 ± 1.41) (Fig 6D). Conversely, absence of the Gli TFBS lifted the strong Gli3-mediated repression of the *rx2* pCRE (0.37 ± 0.01 to 0.56 ± 0.11) (Fig 6D). These results of the *trans*-regulation assays underscore the significance of both identified motifs for the regulation of *rx2* expression through Sox2 and Gli3.

To gain further insight into the molecular mechanism underlying the regulation of *rx2*, we performed chromatin immunoprecipitation (ChIP)-PCR assays. To this end, *rx2* pCRE luciferase plasmids co-expressed with GFP-tagged Sox2 or Gli3 fusion proteins were analyzed by immunoprecipitation of chromatin with antibodies directed against GFP. Subsequent amplification of co-precipitated DNA by qPCR using oligonucleotides flanking the specific TFBSs and the luciferase coding sequence (control), respectively, revealed a specific binding of both factors analyzed to their *in vitro*-validated binding sites. This was indicated by a five- to sevenfold enrichment of the *rx2* pCRE (1st ChIP: 7.71; 2nd ChIP: 5.18) in comparison to the control (Fig 6E) in the Sox2 ChIP. Upon mutation of the Sox motif, this enrichment was severely reduced (1st ChIP: 3.18; 2nd ChIP: 3.03), indicating a specific binding of Sox2 to the predicted binding site *in vivo*. Similarly, Gli3 was binding to the predicted site in the *rx2* pCRE, though with lower affinity (1st ChIP: 1.38; 2nd ChIP: 1.41). In the absence of the binding site (*rx2* pCRE delGli), no input enrichment (1st ChIP: 1.07; 2nd ChIP: 1.10) was detectable, indicating the specificity of the interaction (Fig 6F). Similar results were obtained for the TFs Tlx (Yu *et al*, 1994) and Her9 (Sasai *et al*, 1992), where we could show a direct site-specific binding to the *rx2* pCRE in EMSA (Supplementary Fig S4) and ChIP-PCR (Supplementary Fig S5, Supplementary Table S2), respectively. In summary, our biochemical analysis and transcriptional assays revealed binding sites for the TFs Sox2 and Gli3, which are bound by the corresponding factors in a sequence-specific manner to regulate the activity of the *rx2* pCRE.

Sox2 and Gli3 confine Rx2 expression to adult RSCs through direct protein–DNA interaction

To gain insight into the biological relevance of the predicted and characterized Gli- and Sox-binding sites for *rx2* expression *in vivo*, we introduced the same modifications that impaired physical interaction with the respective TFs. We generated stable transgenic lines (*rx2* pCRE delGli and *rx2* pCRE mtSox) expressing nuclear FPs (Fig 7A) and assayed the impact of Gli3 and Sox2 on Rx2 reporter expression *in vivo*.

Gli is required for confining Rx2 expression to the periphery of the CMZ and at the same time necessary to prevent its expression in the peripheral RPE. Upon interference with Gli binding to the *rx2* pCRE (*rx2*::H_2B-mRFP delGli), *rx2* reporter expression was shifted to the Gli3-expression domain in the RPE (Fig 7C), consistent with Gli3 acting as an *in vivo rx2* repressor (n = 15/15 hatchlings). Simultaneously, *rx2* reporter expression was massively reduced in the peripheral CMZ (Fig 7C–C″), indicating that the single Gli-binding site identified and characterized mediates both activating (CMZ) and repressing (RPE) activities. These data corroborate the *in vitro* findings (above) and highlight their relevance *in vivo*.

The binding of Sox2 is necessary for the expression of *rx2* in the CMZ. Mutation of the Sox-binding site (*rx2*::H_2B-mRFP mtSox) resulted in massive reduction of *rx2* reporter expression in the CMZ, both in terms of levels and cell numbers (Fig 7E–E″) (n = 14/14 hatchlings) compared to controls (*rx2*::H_2B-mRFP) (Fig 7D–D″). Interestingly, the mutation of the Sox-binding site also affected *rx2* reporter expression in Müller glia cells, the only other retinal cell type that co-expresses *sox2* and *rx2*. In contrast, *rx2* mtSox reporter expression was unaffected in post-mitotic photoreceptor cells, which express *rx2*, but not *sox2* (compare Supplementary Fig S6A–A″ to Supplementary Fig S6B–B″).

These results indicate a critical *in vivo* role of the Sox-binding site and its interaction with the TF Sox2 for the onset and maintenance of *rx2* expression in RSCs in the CMZ and in Müller glia cells. Our analyses support a dual role for the TF Gli3 as a direct context-dependent mediator of *rx2* activation and repression, respectively.

Rx2 activity is required for the balance between RPE and neuroretinal stem cells

To ultimately address the role of Rx2 in the retinal stem cells in the peripheral CMZ, we established mutant alleles targeting the *rx2* locus with transcription activator-like effector nucleases (TALENs). Customized TALEN pairs were designed to bind the coding sequence in the homeodomain of the *rx2* gene. Mutations were introduced by injection of mRNA (Ansai *et al*, 2013) encoding the Rx2-specific TALEN pair at the one-cell stage. Successful targeting of the *rx2* locus was validated by PCR and followed by sequence analysis in the injected and subsequent generation. Embryos carrying a homozygous mutation in *rx2* (RNA null) are transiently delayed in retinal development but ultimately develop morphologically normal eyes with slightly reduced eye size (Fig 8A). They are viable and can be maintained as homozygous stock (Fig 8A). The spatiotemporal redundancy of *rx2* expression in comparison to other highly related paralogous genes (*rx3* in RPCs, *rx1* in RSCs) presents a likely argument for the lack of a strong phenotype in mutant fish.

To challenge the capacity of *rx2*-mutant cells to contribute to retinal stem cells, we generated chimeric retinae by transplanting labeled wild-type cells into *rx2*-mutant embryos. When wild-type blastula cells are transplanted into a wild-type blastula host, they contribute to both stem cell populations, either to neuroretinal stem cells or to RPE stem cells as indicated by the formation of NR ArCoS and RPE ArCoS, respectively (34 NR ArCoSs and 13 RPE ArCoSs distributed in eight retinae; NR/RPE ratio = 2.6) (Fig 8B and C). Conversely, in the context of a *rx2*-mutant background, wild-type blastula cells transplanted into a mutant host preferentially give rise to neuroretinal stem cell ArCoSs, and contribute only occasionally to the RPE (24 NR ArCoSs and three RPE ArCoSs distributed in eight retinae; NR/RPE ratio = 8) (Fig 8D). Thus, our mosaic analysis revealed a requirement for Rx2 activity in balancing the contribution to the stem cell pools of neuroretinal stem cells and RPE stem cells. In the absence of Rx2 activity, RPE is preferentially formed, resulting in the exclusion of wild-type contribution in a mosaic situation. These data corroborate the findings presented above and, altogether, highlight an intricate connection between fate determinations of stem cell populations via the activity of Rx2, which ensures the proper balance of the two stem cell populations.

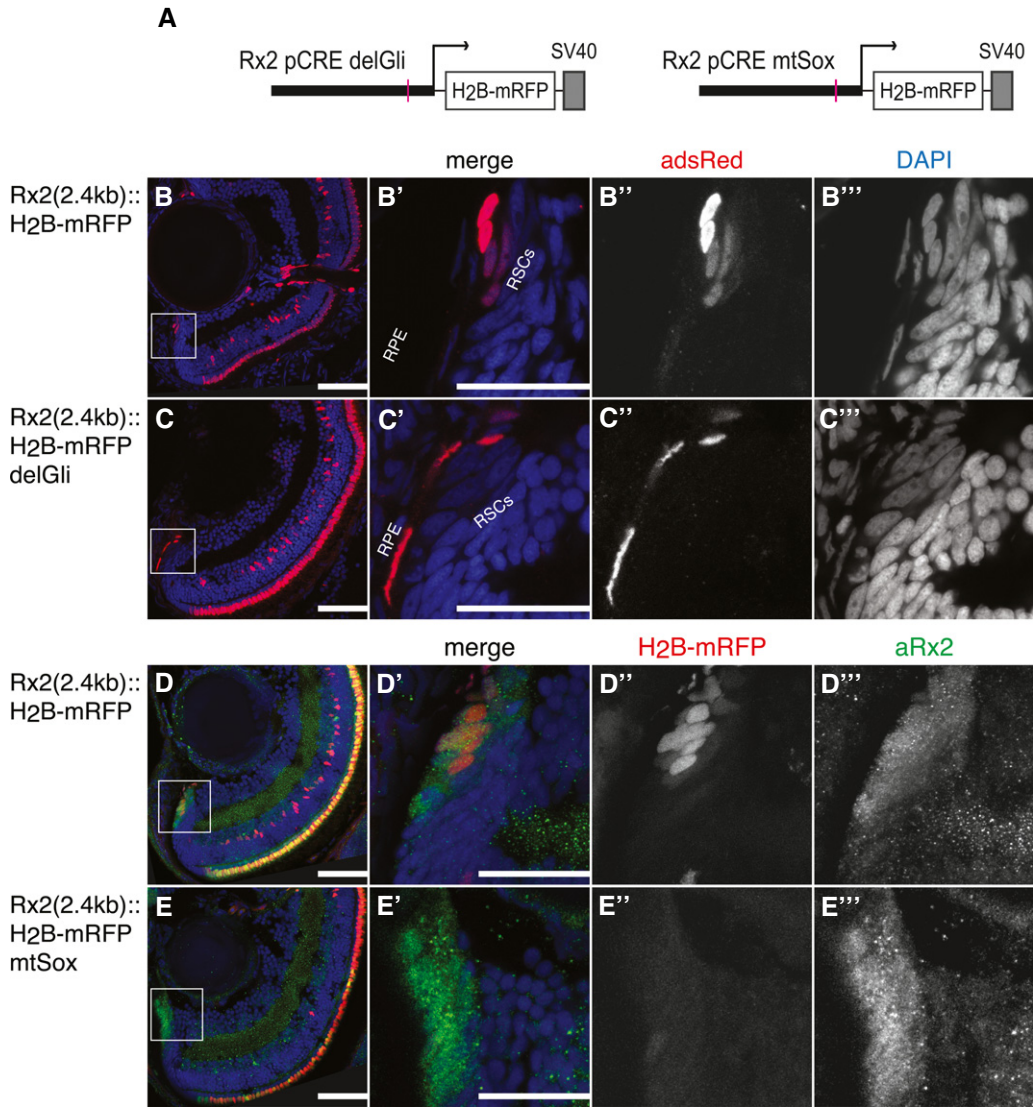

Figure 7. Sox- and Gli-binding sites are crucial for the *rx2 cis*-regulatory activity in the CMZ.

A Transgenic lines carrying the *rx2* pCRE with mutations (indicated by pink bars) in the predicted Gli- (*rx2* pCRE delGli) and Sox-binding site (*rx2* pCRE mtSox) followed by a nuclear FP were generated for *in vivo* validation.

B–C‴ Loss of the Gli-binding site in the *rx2* pCRE generates shift of *rx2* reporter expression into the RPE. Images in (B′–B″) are magnifications of the area boxed in (B), and images in (C′–C‴) are magnifications of the area boxed in (C).

D–E‴ Mutation of Sox-binding site abolishes *rx2 cis*-regulatory activity in the CMZ. Images in (D′–D‴) are magnifications of the area boxed in (D), and images in (E′–E‴) are magnifications of the area boxed in (E).

Data information: RPE, retinal pigmented epithelium; RSCs, retinal stem cells. Scale bars represent 50 μm in (B, C, D, E) and 25 μm in (B′, C′, D′, E′).

Discussion

Here, we identify and characterize the TF *rx2* as a proxy for retinal stem cells with a key function in balancing retinal stem cell populations and establish a scaffold network of directly interacting TFs that control and likely confine *rx2* expression to RSCs *in vivo*. Strikingly, an individual $rx2^+$ cell is a stem cell either for the NR or for the RPE. Each individual $rx2^+$ NSC is multipotent and gives always rise to the full complement of retinal cell types. By identifying upstream regulators of *rx2*, we have gained mechanistic insight into the transcriptional control of retinal stemness. The bifunctional $rx2^+$ stem cell domain within the CMZ is defined by both transcriptional activators (Sox2, Tlx) and transcriptional repressors (Gli3, Her9) (Fig 9A). We hypothesize that the combined activities of those factors confine Rx2 expression and facilitate the balanced establishment of stem cells for the NR and the RPE within the CMZ.

We followed an unbiased approach (Souren *et al*, 2009) to initially identify proteins interacting with the *rx2* CRE *in vitro*. This approach has clear limitations due to the composition of the initially screened gene set and the fact that we only assayed for the activity of individual genes. Nevertheless, we successfully identified key transcriptional regulators of *rx2* that directly interact with the *rx2*

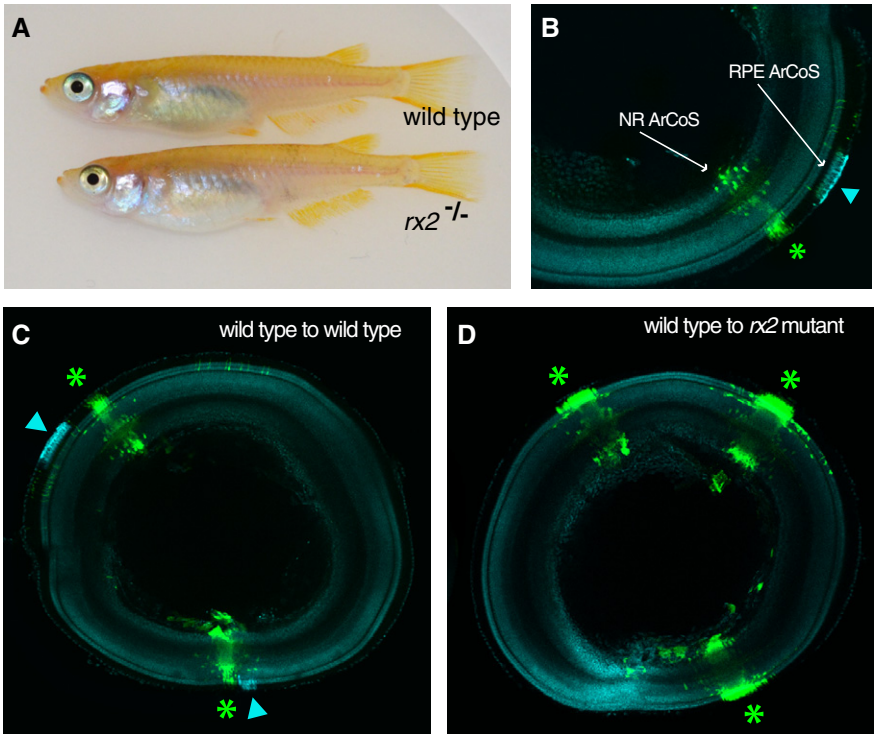

Figure 8. Rx2 balances fate decisions of retinal stem cells.

A Adult wild-type (top) and *rx2* homozygous mutant fish (bottom).

B Transplantation of permanently labeled wild-type cells at the blastula stage into a wild-type host results in the formation of both NR (asterisk, green) and RPE (arrowhead, blue) ArCoSs.

C Control transplantations (wild-type to wild-type).

D Transplantation of wild-type cells into *rx2*-mutant host blastulae results in the preferential formation of NR ArCoSs.

CRE *in vitro* and *in vivo* and exert key functions in confining the $rx2^{+}$ RSCs to the periphery of the CMZ.

Conditional mosaic expression of individual *rx2* activators in the central retina resulted in the de-differentiation of post-mitotic retinal cells and the induction of stem cell features therein. These terminally differentiated cells are efficiently reprogrammed by the combination of Tlx and Sox2, consistent with reports in cultured NSCs, where a direct interaction between Sox2 and Tlx alleviates a negative feedback loop acting on the *tlx* promoter (Shimozaki *et al*, 2012). Additionally, both factors have been shown to be crucial for the maintenance of mammalian NSCs (Bylund *et al*, 2003; Graham *et al*, 2003; Shi *et al*, 2004; Taranova *et al*, 2006; Liu *et al*, 2008). We hypothesize that both factors synergize in the central CMZ to establish the niche for neuroretinal stem cells (Fig 9A).

Our data connect Sox2, Tlx, Gli3, and Her9 forming a core scaffold, which converges on the *rx2* pCRE and modulates *rx2* expression in adult RSCs (Fig 9B). Because these TFs are known to participate in non-exclusive protein–protein interactions (Kageyama *et al*, 2007; Qu & Shi, 2009; Kondoh & Kamachi, 2010), it is possible that a combinatorial code with additional cofactors modulates the spatiotemporal function and activity of the core components of the network. Previous studies in *Xenopus* reported the interdependence of Sox2 and Otx2 for *rx* activation (Danno *et al*, 2008; Martinez-De Luna *et al*, 2010). Even though we failed to detect *Otx2* transcripts in the CMZ (data not shown), we cannot entirely exclude the presence of Otx2 at basal levels in the *trans*-regulation assays. However, the graded response to increasing concentrations of Sox2 strongly argues for a Sox2-mediated *rx2* regulation independent of Otx2. Since fish and amphibia possess the highest regenerative capacity amongst vertebrates and show lifelong, post-embryonic retinogenesis, the difference in *rx* regulation is unexpected. Addressing how the regulatory scaffold presented here has evolved from fish over frogs to mammals will present one aspect toward our understanding of the gradual loss of proliferative and regenerative capacity in the retina of higher vertebrates.

One of the striking findings of this work relates to the fact that a single retinal stem cell expressing *rx2* can either be a multipotential stem cell for the neuroretina or be a stem cell for the RPE. Here, distally adjacent to the CMZ, Gli3 (Fig 9A, blue) acts as repressor, confining *rx2* expression (Fig 9A, red) to the CMZ. The shift of *rx2* reporter expression from the CMZ to the RPE upon deletion of the Gli-binding site underlines a dual function of Gli3: It mediates *rx2* repression in the RPE as well as *rx2* activation in the directly adjacent CMZ. These data together with the fact that *rx2*-mutant cells preferentially contribute to the RPE RSC pool (discussed below) indicate that Rx repression (mediated by Gli 3 in the wild-type retina) is a prerequisite for commitment toward RPE fate.

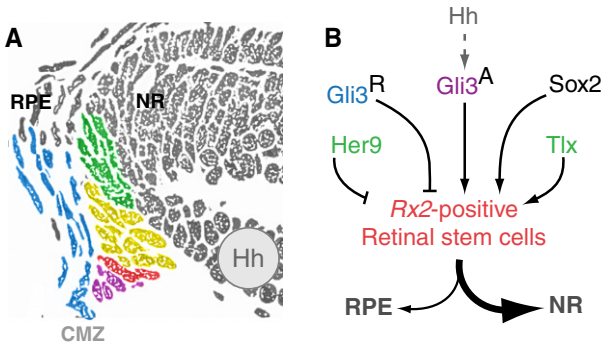

Figure 9. A proposed model summarizing spatial regulation of *rx2* expression and RSC-specific features through *sox2*, *tlx*, *her9*, and *gli3*.

A Schematic illustration outlining the spatial distribution of *rx2* (red), *sox2* (black dashed line), *tlx* (green), *her9* (green), and *gli3* (blue) transcripts in the CMZ and RPE. Purple indicates overlap between *rx2* and *gli3*; yellow indicates overlap between *rx2* and *tlx/her9*.

B RSC-specific gene regulatory network operating *in vivo*. *sox2* (black) and *tlx* (green) directly interact with the *rx2* pCRE to activate *rx2* expression in the CMZ as well as other stem cell features. Her9 (green) restricts *rx2* expression centrally, and Gli3 prevents Rx2 from being expressed in the RPE. Proximity to the hedgehog morphogen (gray) secreted from the ganglion cell layer could dictate the activating function (purple) in the peripheral CMZ and repressive action (blue) in the RPE of Gli3 protein isoforms.

Here, Gli TFs (Fig 9A, purple) function as activators in the presence of a Shh signal (gray) emanating from the RGC layer (Borday *et al*, 2012) and crucially contribute to *rx2* expression at this site. This can be modulated by additional Gli TFs expressed in the CMZ (data not shown) as reported in fish and frog, regulating *rx2* expression via the same evolutionarily conserved motif. Additionally, it has been reported that Gli TFs act as direct transcriptional repressors or activators dependent on the activity of the Hh signaling cascade (Humke *et al*, 2010) (Fig 9B), a pathway shaping the CMZ (Borday *et al*, 2012). While multiple Gli proteins are potentially involved in the regulation of *rx2* expression *in vivo*, no SoxB1 genes other than *sox2* are expressed in the post-embryonic medaka CMZ (not shown). Thus, the activity uncovered for Sox2 and its binding site in the *rx2* pCRE can be unambiguously attributed to Sox2. Recent studies provided evidence for synergistic action between SoxB1 and Gli TFs to activate Shh target genes during neural tube development (Oosterveen *et al*, 2012; Peterson *et al*, 2012). It has been shown that Sox and Gli TFs occupy the same regulatory elements of common targets (Peterson *et al*, 2012). Given the close proximity of the tested Sox and Gli motif in the *rx2* pCRE. A Gli activator could exert its function in concert with Sox2 in the CMZ to activate Rx2 and possibly modulate RSC fate toward the NR. In the RPE, a Gli repressor in the absence of Hh signal could use the same Gli site to restrict *rx2* expression independent of Sox2. Interestingly, non-coding regions bound by Gli1 included a regulatory region of *sox2* in neural progenitors (Peterson *et al*, 2012); therefore, Hh-dependent Gli may help to maintain *sox2* expression in the CMZ in order to keep stem cells and progenitors in an undifferentiated state. The relevance of Gli-mediated repression of rx2 is corroborated by the requirement of rx2 for balancing neuroretinal and RPE fates. In the absence of rx2 (by repression or mutation), RPE fate is strongly favored. Intriguingly, *rx2*-mutant cells display a striking phenotype when challenged with wild-type cells within the same niche. In a mosaic retina, the absence of Rx2 activity favors the formation of RPE and consequently prevents wild-type cells to take RPE stem cell fate. Therefore, our data not only highlight an intricate connection between fate determinations of both stem cell domains via the activity of Rx2. They furthermore also imply a cell non-autonomous feedback activity ensuring a balance of both stem cell populations. The transcriptional confinement of *rx2* to the CMZ by the activity of the regulatory scaffold presented here connects the stem cells of the NR and those of the RPE and thus sheds light on the mechanism specifying this composite stem cell niche.

Materials and Methods

Medaka stocks

Medaka (*Oryzias latipes*) stocks were maintained as previously described (Koster *et al*, 1997). All fish are maintained in the closed stocks of COS at Heidelberg University. Fish husbandry and experiments were performed according to local animal welfare standards (Tierschutzgesetz 111, Abs. 1, Nr. 1, Haltungserlaubnis) and in accordance with European Union animal welfare guidelines. The fish facility is under the supervision of the local representative of the animal welfare agency. Embryos were staged according to Iwamatsu (2004).

Transgenesis

Injections were done as previously described (Rembold *et al*, 2006b). For transient expression, *driver* and *effector* plasmids were co-injected (30 ng/µl final concentration) in two-cell stage medaka embryos (Rembold *et al*, 2006a).

Molecular cloning

LexPR and LexOP cassettes were derived from pDs(*krt8:*LPR-*LOP:*G4) and pDs(*cry:*C-*LOP:*Ch) to generate *driver*, *effector*, or *driver–effector* constructs (Emelyanov & Parinov, 2008). A cassette containing the LexOP operator upstream of the Cherry coding sequence was extracted from pDs*(cry:*C-*LOP:*Ch*)*. The Cherry coding sequence was replaced with H_2B-EGFP and H_2A-Cherry. *Effectors*: *LexOP*::H_2A-Cherry; *LexOP*::H_2B-EGFP; *LexOP*::Cherry. A cassette containing the coding sequence for the LexPR *trans*-activator followed by the LexOP operator was released from pDs*(krt8:*LPR-*LOP:*G4*)* and inserted downstream of the *rx2* pCRE (Inoue & Wittbrodt, 2011). Coding sequences for *gli3* and *her9* were inserted downstream of the LexOP operator. A second LexOP operator followed by H_2B-EGFP coding sequence was added (released from *LexOP*::H2B-EGFP). *Driver–Effectors: rx2*::LexPR *LexOP*::Gli3 *LexOP*::H2B-EGFP; *rx2*::LexPR *LexOP*::Her9 *LexOP*::H_2B-EGFP; *rx2*::LexPR *LexOP*::H_2B-EGFP.

A cassette containing the coding sequence for the LexPR *trans*-activator followed by the LexOP operator was introduced downstream of the *cska* promoter (Grabher *et al*, 2003). Coding sequences for *sox2* and *tlx* were inserted downstream of the LexOP operator. *Drivers: cska*::LexPR *LexOP*::Sox2; *cska*::LexPR *LexOP*::Tlx,*; cska*::LexPR *LexOP*.

The coding sequence of the nuclear FPs in the *rx2*::H_2B-mRFP vector (Inoue & Wittbrodt, 2011) was replaced by tubulin-GFP fusion. The 2.4-kb *rx2* pCRE was released through restriction digest and cloned upstream of the luciferase gene into the pGL4.1 luciferase reporter vector (Promega).

Coding sequences for *sox2*, *gli3*, and *her9* were derived from a full-length cDNA library based on the pCMV-Sport6.1 vector (Souren *et al*, 2009); *tlx* cDNA was derived from a Lambda ZAP cloning vector. Full-length *Olrx2* (NP_001098373.1) for antibody generation was cloned by PCR from medaka stage 32 cDNA using the following primers: forward primer: 5′-GGAATTCCATATGATGCATTTGTC AATGGATAC-3′; reverse primer: 5′- CGGGATCCTCACATGTGCTGC CAGG-3′. PCR products were digested with restriction enzymes NdeI and BamHI, ligated into the *pET15b* (Merk Millipore), which was cleaved with the same enzymes. *pET15b-Olrx2* was used to bacterially express OlRx2 protein as the antigen for generation of OlRx2 antibody.

The 2.4-kb Medaka *rx2* pCRE was cloned in a *pBS/I-SceI* already containing a tamoxifen-inducible Cre recombinase (from pIndu Perfect) resulting in pBS/I-SceI/*rx2*::^{ERT2}CRE/I-SceI. All constructs generated for transient expression or transgenesis were based on a pBluescript plasmid containing two I-SceI sites flanking the insert.

N-terminal mGFP-flexible linker (FL) fusion protein constructs (mGFP-FL-Her9, mGFP-FL-Sox2, and mGFP-FL-Tlx) for ChIP analysis were generated by Golden GATEway (GGW) cloning system (Kirchmaier *et al*, 2013). Routinely, respective genes and FL were cloned into appropriate GGW entry vectors and assembled into GGW destination vectors. These GGW destination vectors were used to clone respective mGFP-FL fusion constructs into pSport6.1 vector. FL was generated by annealing with the sense oligo: GATCCTCCCT GAGCGGTGGAGGCGGTTCAGGCGGAGGTGGCTCTGGCGGTGGCGG ATCGGGAGGCGGTGGAAGTGCAGCCGCGGGTG and the antisense oligo: GTACCACCCGCGGCTGCACTTCCACCGCCTCCCGATCCGCCA CCGCCAGAGCCACCTCCGCCTGAACCGCCTCCACCGCTCAGGGA. For mGFP-FL-Gli3, mGFP-FL was released from the assembled pSport6.1 vectors via restriction digest and inserted upstream of pSport6.1-Gli3.

Trans-regulation screen

Cell culture, transfection, and luciferase readout were carried out with 1,151 cDNA clones representing the majority of the annotated medaka TFs as previously described (Souren *et al*, 2009). For each well, pSport6.1-cDNA (100 ng), *rx2*::luc2 (40 ng), and pRL-CMV (5 ng) were co-transfected.

Site-directed mutagenesis

Amino acid substitutions or deletions were introduced into the *rx2* gene regulatory region of *rx2*::H_2B-mRFP by site-directed mutagenesis (Quikchange, Stratagene) using the following primers: putative Sox-binding site, forward primer: 5′-CCACACAAGCCATTATCTTT CAGACGCTAGATTTGTTGAAAGGAAGTTTTGT-3′; reverse primer: 5′-ACAAAACTTCCTTTCAACAAATCTAGCGTCTGAAAGATAATGGC TTGTGTGG-3′; Gli-binding site, forward primer: 5′-GAAGTTTT GTTGAGGCTTCATTAGCAATGTGGTCTGAAAGCAG-3′; and reverse primer: 5′-CTGCTTTCAGACCACATTGCTAATGAAGCCTCAACAAA ACTTC-3′.

In vitro translation and EMSA

Medaka Sox2, Tlx, Gli3, and Her9 proteins were generated from cDNA clones by *in vitro* transcription and translation using the TNT Quick Coupled Transcription/Translation System (Promega). Complementary oligonucleotides were annealed in annealing buffer (10 mM Tris–HCl, pH 8.0, 50 mM NaCl, 1 mM EDTA). Biotin-labeled oligonucleotides (25 fmol) were incubated with 5 µl protein translation reaction for 1 h at 4°C in binding buffer (for Gli3 and Tlx: 10 mM Tris, 1 mM DTT, 5 mM $MgCl_2$, 5% glycerol, 1 mM EDTA, 0.05% NP-40, and 50 ng/µl poly(dI-dC); for Sox2 and Her9: 10 mM Tris, 1 mM DTT, 2.5 mM $MgCl_2$, 100 mM KCl, 5% glycerol, 1 mM EDTA, 0.05% NP-40, and 50 ng/µl poly(dI-dC)) in 20 µl total volume.

The binding reactions were subjected to electrophoresis on a pre-run native 6% polyacrylamide gel in 0.5× TBE. Signal was detected using the LightShift Chemiluminescent EMSA kit (Thermo Scientific) according to the manufacturer's instructions. Oligonucleotide sequences used are summarized in Supplementary Table S3.

Dose–response assay

pGL4.1 vector containing the *rx2* pCRE with different mutations (40 ng) and pRL-*CMV* vector (5 ng) were co-transfected with 20, 40, 80 or 160 ng of medaka cDNA (pSport6.1-cDNA) per well. A total amount of 205 ng DNA was transfected in each well through addition of empty pCS2+ vector. The assays were carried out in quadruplicate.

Chromatin immunoprecipitation

ChIPs were performed with the SimpleChIP Enzymatic Chromatin IP kit (New England Biolabs) according to the manufacturer's instructions. BHK cells were co-transfected with 6 mg pGL4.1-*rx2* and 3 mg pSport6.1-mGFP-FL-cDNA. Chromatin was incubated with 20 µl of agarose beads attached to anti-GFP antibodies (Chromotek) at 4°C overnight. Quantification of DNA by PCR was carried out in a thermocycler (Bio-Rad) using ABsolute qPCR SYBR Green Mix (Thermoscientific). Primers used to amplify regions containing putative binding sites within the *rx2* pCRE and control primers for firefly luciferase coding sequence are summarized in Supplementary Table S4. Two independent biological replicates were carried out for each genomic region of interest. Each qPCR was performed as duplicates.

Whole-mount *in situ* hybridization

For anti-sense riboprobe synthesis, linear templates were produced from full-length cDNA clones either through standard PCR (*sox2*, *gli3* and *her9*) or restriction enzyme digestion 5′ of the start codon (*rx2* and *tlx*). T7 RNA polymerase-based transcription was carried out as previously described (Loosli *et al*, 1998). Fluorescent whole-mount *in situ* hybridizations were performed as previously described (Schuhmacher *et al*, 2011). Signals were detected using TSA-Plus Fluorescein and Cyanine 5 Systems (Perkin Elmer). For combined single-color fluorescent whole-mount *in situ* hybridization and immunostaining, embryos were incubated for 2 days with anti-fluorescein antibody conjugated to horseradish peroxidase (Roche)

and anti-GFP antibody (Invitrogen) at 4°C. After riboprobe detection using TSA-Plus Cyanine 3 System (Perkin Elmer), the embryos were incubated with fluorescent-conjugated secondary antibody and 4′,6-diamidino-2-phenylindole (DAPI, 1:500, Sigma) for 2 days at 4°C. Whole-mount *in situ* hybridizations using NBT/BCIP detection were carried out as previously described (Loosli *et al*, 1998). 25-μm-thick sections were obtained using a VT1000S vibratome (Leica) after mounting stained embryos in 4% agarose (Sigma).

Immunohistochemistry

16-μm cryosections and immunostainings were preformed as previously described (Inoue & Wittbrodt, 2011). When necessary, cryosections were subjected to 3% H_2O_2 in 1% KOH for 30 min prior to immunostainings. Anti-OlRx2 antibody was raised against the full-length OlRx2 (NP_001098373.1) recombinant protein in rabbits (Charles River), and affinity-purified as described previously (Barenz *et al*, 2013). Primary antibodies used were rabbit anti-phospho-histone H3 (1:500; Upstate), mouse anti-PCNA (1:100; Santa Cruz), rabbit anti-OlRx2 (1:500), chicken anti-GFP (1:500, Invitrogen), rabbit anti-DsRed (1:250, Clontech), mouse anti-BrdU (1:50, Becton Dickinson), mouse anti-Islet (1:250, DSHB), mouse anti-GS antibody (1:50, Chemicon), and anti-chicken, anti-mouse, or anti-rabbit fluorescent secondary antibodies (1:1,000, DyLight488, DyLight549 and DyLight647, Jackson). Cell nuclei were counterstained with DAPI. For BrdU detection, cryosections were dried overnight, rehydrated with 1× PTW (1× PBS pH 7.3, 0.1% Tween) and treated with 2 N HCl for 90 min, and then blocked with 10% sheep serum (Sigma).

BrdU treatment

Embryos were incubated in a solution of 1 g/l BrdU for 3 days and fixed immediately afterward in 4% paraformaldehyde.

RU486 treatment

Mifepristone (Sigma, Tocris, Cayman) was dissolved in dimethylsulfoxide (DMSO) to a final concentration of 25 mM and stored as stock solution at −20°C. The stock solution was added to the medium and used at final concentrations up to 20 μM.

Tamoxifen treatment

Tamoxifen was used at a concentration of 2.5 mM (T5648, Sigma) and applied for 12–24 h. Embryos were washed several times after the treatment. A 50 mM stock solution in DMSO was stored at −20°C.

Establishment of *rx2*-mutant alleles

The TALENs designed to bind the *Rx2* coding sequence (Jean-Paul Concordet) were provided in pCS2+ backbones with the following DNA-binding domains: N106: TCGAGAAGTCCCACTA; N107: TCG TTGCCAGTTCCTC.

In vitro mRNA transcription:

Supercoiled DNA of the pCS2+ plasmid was subjected to restriction digest with NotI and the linearized DNA template was purified using the innuPREP PCRpure kit (Analytik Jena) according to the manufacturer's protocol. TALEN N106 and N107 mRNA *in vitro* transcription was performed using the mMessage machine (SP6, Ambion) according to the manufacturer's protocol. The mRNA was purified using the RNeasy RNA purification kit (Qiagen) according to the manufacturer's protocol and stored at −80°C.

mRNAs encoding TALENs directed against the *rx2* coding sequence were injected at the one-cell stage as described for medaka (Ansai *et al*, 2013). To identify mutations in the locus, fin clip DNA of F1 fish was analyzed. The regions of interest for the rx2 TALEN pair were amplified from the isolated genomic DNA with the following primers: *rx2* forward primer: 5′-AACAGTGAGTAGCGGGTCGT-3′; reverse primer: 5′-TCTGAGGGATGGAATTCTGG-3′. The PCR amplification was performed with a proofreading polymerase: 30 s 98°C; (20 s 98°C, 45 s 67°C, 45 s 72°C) repeated for 29 cycles, 5 min followed by 72°C; and followed by 15 min at 72°C with Taq polymerase. The resulting PCR product (930 bp) was enzymatically digested with HpaII. Uncleaved fragments resulting from TALEN-induced mutations in the HpaII recognition site were purified, cloned, and validated by sequencing. RNA null alleles were crossed to homozygosity and maintained as homozygous stock. Stocks are validated each generation by allele-specific PCR on fin clip DNA. Wild-type *rx2* alleles were identified with the following primers: forward primer: 5′-GGGGATTGATGGAGATGGAGT-3′; reverse primer: 5′-CGGCTGTAGACGTCTGGA-3′.

Mutant *rx2* alleles were identified with the following primers: forward primer: 5′-GGGGATTGATGGAGATGGAGT-3′; reverse primer: 5′-CCTCCCGTCTGGATAGTGG-3′.

Transplantation experiments

Transplantations were performed as previously described (Ho & Kane, 1990; Rembold *et al*, 2006a). For experiments in Fig 1, homozygous *Wimbledon* males (Centanin *et al*, 2011) were crossed to heterozygous *rx2*::H_2B-mRFP females; 10–15 blastula cells from the progeny (100% *Wimbledon*$^{+/-}$, 50% *rx2*::H_2B-mRFP$^{+/}$) were transplanted to the central part of wild-type (Cab strain) blastulae. Transplanted embryos were kept in agar-coated dishes in 1xERM supplemented with penicillin–streptomycin (1:200, Sigma) and selected for GFP$^+$, RFP$^+$ cells in the retina.

For experiments shown in Fig 8, heterozygous *Wimbledon* males were crossed to wild-type females; 20–30 blastula cells from the progeny were transplanted to the central part of either *rx2*-mutant or a wild-type blastulae. Transplanted embryos were raised in agar-coated dishes in 1× ERM supplemented with penicillin–streptomycin (1:200, Sigma), selected for GFP$^+$ clones in the retina 5 days post-transplantation and grown to the desired age for ArCoS analysis.

Imaging

Samples were imaged using an Olympus MVX10 binocular coupled to a Leica DFC500 camera, a Nikon AZ100 coupled to a Nikon C1 (entire retinae), or a Leica TCS SPE (sections). Images of NBT/BCIP stainings were taken using a Leica DM5000 scope equipped with a Leica DFC500 camera. For cell counting, an automated segmentation tool (maximum entropy threshold) for ImageJ (Version 1.41o; http://rsbweb.nih.gov/ij/) was used.

Supplementary information for this article is available online: http://emboj.embopress.org

Acknowledgements

We thank N. Foulkes, S. Lemke, F. Loosli, and J.L. Mateo for critical discussion and comments on the manuscript; J.L. Mateo and M. Ramialison for help with the DNA motif analysis; M. Gebert for advice regarding the EMSA; E. Leist and A. Saraceno for fish husbandry; and T. Kellner and L. Schertel for technical assistance. DI received fellowships from the Human Frontier Science Program (HFSP) and the Japan Society for the Promotion of Science (JSPS); TT received a fellowship of the Hartmut Hoffmann Berling International Graduate School (HBIGS) in Heidelberg. The project was supported by the Collaborative Research Center SFB 873 (J.W.) of the German Research Foundation (DFG).

Author contributions

RR (*in vivo*, *in vitro* and cell culture assays, generation of *rx2* mutants) and LC (lineage-tracing analysis, transplantation assays) performed the experiments with contributions from TT (transplantation assays), DI (Rx2 antibody and GFP fusion proteins), J-PC (design of *rx2* talens) BW (*rx2* mutants), and JRM-M (*rx2*::Tub-GFP transgenic line). RR, LC, TT and JW designed the experiments and analyzed the data. RR, LC and JW wrote the manuscript with contributions from DI, TT and JRM-M.

Conflict of interest

The authors declare that they have no conflict of interest.

References

Adolf B, Chapouton P, Lam CS, Topp S, Tannhäuser B, Strähle U, Götz M, Bally-Cuif L (2006) Conserved and acquired features of adult neurogenesis in the zebrafish telencephalon. *Dev Biol* 295: 278 – 293

Amato MA, Arnault E, Perron M (2004a) Retinal stem cells in vertebrates: parallels and divergences. *Int J Dev Biol* 48: 993 – 1001

Amato MA, Boy S, Perron M (2004b) Hedgehog signaling in vertebrate eye development: a growing puzzle. *Cell Mol Life Sci* 61: 899 – 910

Ansai S, Sakuma T, Yamamoto T, Ariga H, Uemura N, Takahashi R, Kinoshita M (2013) Efficient targeted mutagenesis in medaka using custom-designed transcription activator-like effector nucleases. *Genetics* 193: 739 – 749

Barenz F, Inoue D, Yokoyama H, Tegha-Dunghu J, Freiss S, Draeger S, Mayilo D, Cado I, Merker S, Klinger M, Hoeckendorf B, Pilz S, Hupfeld K, Steinbeisser H, Lorenz H, Ruppert T, Wittbrodt J, Gruss OJ (2013) The centriolar satellite protein SSX2IP promotes centrosome maturation. *J Cell Biol* 202: 81 – 95

Borday C, Cabochette P, Parain K, Mazurier N, Janssens S, Tran HT, Sekkali B, Bronchain O, Vleminckx K, Locker M, Perron M (2012) Antagonistic cross-regulation between Wnt and Hedgehog signalling pathways controls post-embryonic retinal proliferation. *Development* 139: 3499 – 3509

Bylund M, Andersson E, Novitch BG, Muhr J (2003) Vertebrate neurogenesis is counteracted by Sox1-3 activity. *Nat Neurosci* 6: 1162 – 1168

Cavallaro M, Mariani J, Lancini C, Latorre E, Caccia R, Gullo F, Valotta M, DeBiasi S, Spinardi L, Ronchi A, Wanke E, Brunelli S, Favaro R, Ottolenghi S, Nicolis SK (2008) Impaired generation of mature neurons by neural stem cells from hypomorphic Sox2 mutants. *Development* 135: 541 – 557

Centanin L, Hoeckendorf B, Wittbrodt J (2011) Fate restriction and multipotency in retinal stem cells. *Cell Stem Cell* 9: 553 – 562

Centanin L, Ander JJ, Hoeckendorf B, Lust K, Kellner T, Kraemer I, Urbany C, Hasel E, Harris WA, Simons BD, Wittbrodt J (2014) Exclusive multipotency and preferential asymmetric divisions in post-embryonic neural stem cells of the fish retina. *Development* 141: 3472 – 3482

Cerveny KL, Cavodeassi F, Turner KJ, de Jong-Curtain TA, Heath JK, Wilson SW (2010) The zebrafish flotte lotte mutant reveals that the local retinal environment promotes the differentiation of proliferating precursors emerging from their stem cell niche. *Development* 137: 2107 – 2115

Danno H, Michiue T, Hitachi K, Yukita A, Ishiura S, Asashima M (2008) Molecular links among the causative genes for ocular malformationtion: Otx2 and Sox2 coregulate Rax expression. *Proc Natl Acad Sci USA* 105: 5408 – 5413

Del Bene F, Ettwiller L, Skowronska-Krawczyk D, Baier H, Matter J-M, Birney E, Wittbrodt J (2007) *In vivo* validation of a computationally predicted conserved Ath5 target gene set. *PLoS Genet* 3: 1661 – 1671

Emelyanov A, Parinov S (2008) Mifepristone-inducible LexPR system to drive and control gene expression in transgenic zebrafish. *Dev Biol* 320: 113 – 121

Grabher C, Henrich T, Sasado T, Arenz A, Wittbrodt J, Furutani-Seiki M (2003) Transposon-mediated enhancer trapping in medaka. *Gene* 322: 57 – 66

Graham V, Khudyakov J, Ellis P, Pevny L (2003) SOX2 functions to maintain neural progenitor identity. *Neuron* 39: 749 – 765

Ho RK, Kane DA (1990) Cell-autonomous action of zebrafish spt-1 mutation in specific mesodermal precursors. *Nature* 348: 728 – 730

Humke EW, Dorn KV, Milenkovic L, Scott MP, Rohatgi R (2010) The output of Hedgehog signaling is controlled by the dynamic association between suppressor of fused and the Gli proteins. *Genes Dev* 24: 670 – 682

Inoue D, Wittbrodt J (2011) One for all–a highly efficient and versatile method for fluorescent immunostaining in fish embryos. *PLoS ONE* 6: e19713

Iwahara N, Hisahara S, Hayashi T, Horio Y (2009) Transcriptional activation of NAD^+-dependent protein deacetylase SIRT1 by nuclear receptor TLX. *Biochem Biophys Res Commun* 386: 671 – 675

Iwamatsu T (2004) Stages of normal development in the medaka Oryzias latipes. *Mech Dev* 121: 605 – 618

Johns PR (1977) Growth of the adult goldfish eye. III. Source of the new retinal cells. *J Comp Neurol* 176: 343 – 357

Kageyama R, Ohtsuka T, Kobayashi T (2007) The Hes gene family: repressors and oscillators that orchestrate embryogenesis. *Development* 134: 1243 – 1251

Kirchmaier S, Lust K, Wittbrodt J, Studies CfO (2013) Golden gateway cloning – a combinatorial approach to generate fusion and recombination constructs. *PLoS ONE* 8: e76117

Kondoh H, Kamachi Y (2010) SOX-partner code for cell specification: regulatory target selection and underlying molecular mechanisms. *Int J Biochem Cell Biol* 42: 391 – 399

Koster R, Stick R, Loosli F, Wittbrodt J (1997) Medaka spalt acts as a target gene of hedgehog signaling. *Development* 124: 3147 – 3156

Lamba D, Karl M, Reh T (2008) Neural regeneration and cell replacement: a view from the eye. *Cell Stem Cell* 2: 538 – 549

Liu H-K, Belz T, Bock D, Takacs A, Wu H, Lichter P, Chai M, Schutz G (2008) The nuclear receptor tailless is required for neurogenesis in the adult subventricular zone. *Genes Dev* 22: 2473 – 2478

Locker M, Agathocleous M, Amato MA, Parain K, Harris WA, Perron M (2006) Hedgehog signaling and the retina: insights into the mechanisms controlling the proliferative properties of neural precursors. *Genes Dev* 20: 3036 – 3048

Loosli F, Köster RW, Carl M, Krone A, Wittbrodt J (1998) Six3, a medaka homologue of the Drosophila homeobox gene sine oculis is expressed in the anterior embryonic shield and the developing eye. *Mech Dev* 74: 159 – 164

Loosli F, Winkler S, Wittbrodt J (1999) Six3 overexpression initiates the formation of ectopic retina. *Genes Dev* 13: 649 – 654

Martinez-De Luna RI, Moose HE, Kelly LE, Nekkalapudi S, El-Hodiri HM (2010) Regulation of retinal homeobox gene transcription by cooperative activity among cis-elements. *Gene* 467: 13 – 24

Martinez-Morales JR, Rembold M, Greger K, Simpson JC, Brown KE, Quiring R, Pepperkok R, Martin-Bermudo MD, Himmelbauer H, Wittbrodt J (2009) Ojoplano-mediated basal constriction is essential for optic cup morphogenesis. *Development* 136: 2165 – 2175

Monaghan AP, Grau E, Bock D, Schütz G (1995) The mouse homolog of the orphan nuclear receptor tailless is expressed in the developing forebrain. *Development* 121: 839 – 853

Moshiri A, Close J, Reh TA (2004) Retinal stem cells and regeneration. *Int J Dev Biol* 48: 1003 – 1014

Oosterveen T, Kurdija S, Alekseenko Z, Uhde CW, Bergsland M, Sandberg M, Andersson E, Dias JM, Muhr J, Ericson J (2012) Mechanistic differences in the transcriptional interpretation of local and long-range Shh morphogen signaling. *Dev Cell* 23: 1006 – 1019

Peterson KA, Nishi Y, Ma W, Vedenko A, Shokri L, Zhang X, McFarlane M, Baizabal J-M, Junker JP, van Oudenaarden A, Mikkelsen T, Bernstein BE, Bailey TL, Bulyk ML, Wong WH, McMahon AP (2012) Neural-specific Sox2 input and differential Gli-binding affinity provide context and positional information in Shh-directed neural patterning. *Genes Dev* 26: 2802 – 2816

Qu Q, Shi Y (2009) Neural stem cells in the developing and adult brains. *J Cell Physiol* 221: 5 – 9

Quiring R, Wittbrodt B, Henrich T, Ramialison M, Burgtorf C, Lehrach H, Wittbrodt J (2004) Large-scale expression screening by automated whole-mount *in situ* hybridization. *Mech Dev* 121: 971 – 976

Raymond PA, Barthel LK, Bernardos RL, Perkowski JJ (2006) Molecular characterization of retinal stem cells and their niches in adult zebrafish. *BMC Dev Biol* 6: 36

Rembold M, Lahiri K, Foulkes NS, Wittbrodt J (2006a) Transgenesis in fish: efficient selection of transgenic fish by co-injection with a fluorescent reporter construct. *Nat Protoc* 1: 1133 – 1139

Rembold M, Loosli F, Adams RJ, Wittbrodt J (2006b) Individual cell migration serves as the driving force for optic vesicle evagination. *Science* 313: 1130 – 1134

Sasai Y, Kageyama R, Tagawa Y, Shigemoto R, Nakanishi S (1992) Two mammalian helix-loop-helix factors structurally related to Drosophila hairy and enhancer of split. *Genes Dev* 6: 2620 – 2634

Sasaki H, Hui C, Nakafuku M, Kondoh H (1997) A binding site for Gli proteins is essential for HNF-3beta floor plate enhancer activity in transgenics and can respond to Shh *in vitro*. *Development* 124: 1313 – 1322

Schuhmacher L-N, Albadri S, Ramialison M, Poggi L (2011) Evolutionary relationships and diversification of barhl genes within retinal cell lineages. *BMC Evol Biol* 11: 340

Shi Y, Chichung Lie D, Taupin P, Nakashima K, Ray J, Yu RT, Gage FH, Evans RM (2004) Expression and function of orphan nuclear receptor TLX in adult neural stem cells. *Nature* 427: 78 – 83

Shimozaki K, Zhang C-L, Suh H, Denli AM, Evans RM, Gage FH (2012) SRY-box-containing gene 2 regulation of nuclear receptor tailless (Tlx) transcription in adult neural stem cells. *J Biol Chem* 287: 5969 – 5978

Sinn R, Peravali R, Heermann S, Wittbrodt J (2014) Differential responsiveness of distinct retinal domains to Atoh7. *Mech Dev* 133: 218 – 229

Souren M, Martinez-Morales JR, Makri P, Wittbrodt B, Wittbrodt J (2009) A global survey identifies novel upstream components of the Ath5 neurogenic network. *Genome Biol* 10: R92

Suh H, Consiglio A, Ray J, Sawai T, D'Amour KA, Gage FH (2007) *In vivo* fate analysis reveals the multipotent and self-renewal capacities of $Sox2^+$ neural stem cells in the adult hippocampus. *Stem Cell* 1: 515 – 528

Sun G, Yu RT, Evans RM, Shi Y (2007) Orphan nuclear receptor TLX recruits histone deacetylases to repress transcription and regulate neural stem cell proliferation. *Proc Natl Acad Sci USA* 104: 15282 – 15287

Taranova OV, Magness ST, Fagan BM, Wu Y, Surzenko N, Hutton SR, Pevny LH (2006) SOX2 is a dose-dependent regulator of retinal neural progenitor competence. *Genes Dev* 20: 1187 – 1202

Yu RT, McKeown M, Evans RM, Umesono K (1994) Relationship between Drosophila gap gene tailless and a vertebrate nuclear receptor Tlx. *Nature* 370: 375 – 379

Zhao C, Deng W, Gage FH (2008) Mechanisms and functional implications of adult neurogenesis. *Cell* 132: 645 – 660